FERMILAB-PUB-18-042-TD
ACCEPTED

Two-Layer 16 Tesla Cosθ Dipole Design for the FCC

Eddie Frank Holik, Giorgio Ambrosio, Giorgio Apollinari

***Abstract*—The Future Circular Collider or FCC is a study aimed at exploring the possibility to reach 100 TeV total collision energy which would require 16 tesla dipoles. Upon the conclusion of the High Luminosity Upgrade, the US LHC Accelerator Upgrade Project in collaboration with CERN will have extensive Nb_3Sn magnet fabrication experience. This experience includes robust Nb_3Sn conductor and insulation scheming, 2-layer cos2θ coil fabrication, and bladder-and-key structure and assembly. By making improvements and modification to existing technology the feasibility of a two-layer 16 tesla dipole is investigated. Preliminary designs indicate that fields up to 16.6 tesla are feasible with conductor grading while satisfying the HE-LHC and FCC specifications. Key challenges include accommodating high-aspect ratio conductor, narrow wedge design, Nb_3Sn conductor grading, and especially quench protection of a 16 tesla device.**

***Index Terms*—Superconducting magnets, Accelerator magnets, Niobium-tin**

I. Introduction

OVER the past 20 years, Nb_3Sn as a conductor and magnet technology has progressed to the point of application in an accelerator [1]. The LHC Accelerator Research Program or LARP in collaboration with CERN has developed and will soon begin production on MQXF Low-β quadrupoles and MBH 11-tesla dipoles as the backbone of the LHC Hi-Lumi upgrade [2].

Upon the conclusion of the Hi-Lumi LHC upgrade, MQXF Nb_3Sn magnet technology will provide a wealth of experience in both design and fabrication that should feed into the next generation accelerator. EuroCirCol is a conceptual design study for a Future Circular Collider sponsored by the European Community soliciting designs for 16 tesla dipoles [3]-[4]. This paper is a preliminary effort to leverage the significant two-layer, Nb_3Sn quadrupole technology developed by LARP toward a 16 tesla dipole. A two-layer dipole has the advantage of reduced tooling, fewer magnet components, roughly half the total turns, winding time, and number of coils. These features combine to possibly reduce cost, risk, and schedule and are the principal arguments for investigating a two-layer design. LARP experience includes 1 meter length Technology Quads with a bore size of 90 mm [5]-[6] and scale up to 3.7 meters with the LQ [7]. The bore size in the high field quadrupole, HQ, was increased to 120 mm as the primary test bed for the full 150-mm-aperture MQXF [8]. Key quadrupole coil features include a spliceless two-layer coil design with plasma coated end parts and curing process to aid fabrication [8], braided on S-2 glass insulation and silane sizing [9], and provisions to accommodate and tune cable dimensional change during reaction [10]-[11].

To place all feasible designs on an equal playing field, the EuroCirCol has standardized the dipole specifications summarized in Table I [12]-[13]. The only non-conformity to the EuroCir specification is the nominal current where 28 kA is needed and <20 kA is specified. The additional current is needed to enable a two-layer design. All other preliminary EuroCirCol designs have 4 or more layers including the cos-theta [14], the block [15], the common-coil [16]-[17], and the canted-cos-theta models [18]. This also will require an internal

TABLE I
EuroCirCol Specifications and Two-Layer Dipole Parameters

	EuroCirCol Specification	LARP type Dipole
Nominal aperture field	16 tesla	16 tesla
Aperture diameter	50 mm	50 mm
Yoke outer diameter	<800 mm	650 mm
Operating point on load line	86%	86%
Nominal current	**<20 kA**	**27.8 kA**
Operating temperature	1.9 K	1.9 K
Cable insulation thickness	0.15 mm	0.15 mm
Inter-layer insulation thickness	0.5 mm	0.6 mm
Ground insulation thickness	2 mm	2 mm
Field Quality reference radius	17 mm	17 mm
Geometric 2-D multipoles	$\leq 3{\cdot}10^{-4}$	$\leq 2.9{\cdot}10^{-4}$
Quench peak temp. (105% I_{nom})	350 K	336 K
Quench peak volt. (105% I_{nom})	1.2 kV	1.1 kV (15 m)
Protection circuit delay	40 ms	40 ms
J_c (16 tesla, 1.9 Kelvin) A/mm^2	**2300**	[a]**1921** [19-20]
Cabling Degradation	3%	3%
Strand diameter	$d < 1.2$ mm	$d < 1.15$ mm
Cable Compaction $c = 1 - w/2d$ (w = cable minor edge width)	$c > 0.14$	[b]0.12 after HT [b]0.15 before HT
Cu/nonCu	>0.8	>1.0
Protection circuit delay	40 ms	40 ms

[a]Actual J_c measurements were taken at 4.2 K.
[b]Cable expansion during heat treatment reduces the apparent compaction.

This work was supported by the U.S. Department of Energy, Office of Science, Office of High Energy Physics, through the US LHC Accelerator Research Program (LARP) and by the High Luminosity LHC project at CERN. The U.S. Government retains and the publisher, by accepting the article for publication, acknowledges that the U.S. Government retains a non-exclusive, paid-up, irrevocable, world-wide license to publish or reproduce the published form of this manuscript, or allow others to do so, for U.S. Government purposes.

E.F. Holik is with the Angelo State University, San Angelo, TX 76904 USA, and also with the Fermi National Accelerator Laboratory, Batavia, IL 60510 USA (e-mail: eholik@fnal.gov).

G. Ambrosio and G. Apollinari are with the Fermi National Accelerator Laboratory, Batavia, IL 60510 USA (e-mail: giorgioa@fnal.gov; apollina@fnal.gov).

This document was prepared by LARP collaboration using the resources of the Fermi National Accelerator Laboratory (Fermilab), a U.S. Department of Energy, Office of Science, HEP User Facility. Fermilab is managed by Fermi Research Alliance, LLC (FRA), acting under Contract No. DE-AC02-07CH11359.

splice, handling of a characteristically large high-field Rutherford cable, and new wedge technology which are briefly addressed but will be part of the necessary continued R&D.

II. Conductor

The Conductor Development Program (CDP) has significantly progressed internal tin Nb_3Sn and currently provides the highest isotropic engineering current density at low temperature. The highest performing conductor available today is RRP® Nb_3Sn strand as fabricated by Oxford Superconducting Technology, a company of Bruker Energy and Supercon Technologies. Recent work at the Applied Superconductivity Center in Tallahassee has engineered an extended heat treatment (350°C/400h, 620°C/600h) that has produced current densities that are only 16% lower than the projected FCC current density [19]-[20]. In keeping with the spirit of LARP/CDP technology, this 'Best Available' conductor will be employed hereafter with properties described in Table I and Fig. 1.

As a further restriction, this design also accounts for measured conductor dimensional change as characterized in MQXF [10]-[11]. MQXF Rutherford cable expands in thickness by 3.5% and in width by 1% which is slightly more than 4.5% expansion in volume. This anisotropic expansion during reaction artificially reduces the cable compaction factor, c, given in the equation below.

$$c = 1 - w/2d \quad (1)$$

In equation (2) w is the cable width and d is the strand diameter. MQXF first generation conductor has an as-cabled compaction of 0.15 with negligible reduction in performance for RRP® strand. To enable powder-in-tube type strand the as-cabled compaction factor was reduced to 0.14. After reaction and conductor expansion the compaction factor reduces to 0.13 and 0.12 for first and second generation MQXF cable. This implies that for designers to use a cable compaction of 1.4 as specified, the as-cabled conductor could have a cable compaction of 1.6 or above 'proven safe' territory for RRP®. The LARP dipole assumes identical cable compaction and expansion from first generation MQXF conductor. All cable parameters are described in Table II.

TABLE II
Magnet and Conductor Parameters

Parameter	Values (H.F./L.F.)	Unit
Strand diameter	1.143/0.943	mm
Number strands	60/60	
Unreacted Minor Edge	1.943/1.603	mm
Unreacted Major Edge	2.165/1.787	mm
Reaction Thickness Expansion	3.5%	
Unreacted Cable Width	38.402/31.985	mm
Reaction Width Expansion	1.0%	
Cu/nonCu ratio	1.04/1.71	
Nominal Current (I_{nom})	27840	A
Load line operational point	86%/86%	
Temperature Margin	3.6/3.7	K
Cu current density	934/1092	A/mm^2
Non-Cu current density	876/1694	A/mm^2
Peak field (I_{nom})	16.22/13.65	T
Peak Voltage to ground	1109	V
Magnet Length	15	m
Stored Energy (105% I_{nom})	1.85	MJ/m
Inductance (105% I_{nom})	4.68	mH/m
Number of Turns (one coil)	14/36	
Quench peak temp. (105% I_{nom})	198/336	K
MIITs (105% I_{nom})	139.5	10^6 A^{2}sec
Protection circuit delay	40	ms

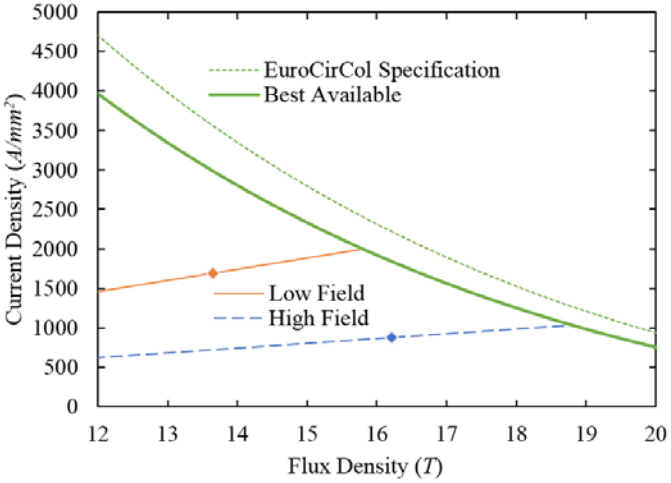

Fig. 1. Superconductor critical current density at 1.9 K. The EuroCirCol Specification is included for reference. The Best Available measured critical current density employs a hyperextended, reduced-temperature Nb_3Sn formation plateau. The Low Field and High Field operational points are included at 86% of Short sample.

III. Cross-Section Design

A. Magnetic Configuration

For this preliminary design, a solid flux return and single bore was used with an inner iron radius of 125 mm and an outer radius of 650 mm. This would allow a collaring structure of roughly 28 mm thickness.

The design specification on cable compaction places a minimum thickness of the cable minor edge. Obtaining 16 tesla with two layers of conductor and minor edge thickness restriction results in non-traditional block rotation. To maintain

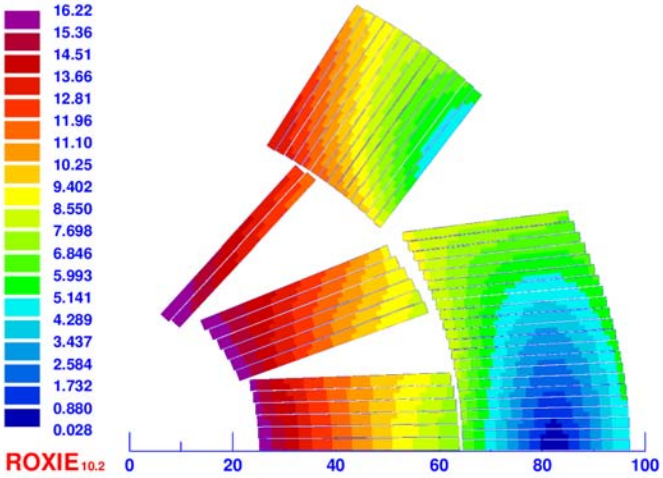

Fig. 2. Field distribution including self-field of one quadrant of the optimized two-layer dipole. The bore field is 16.0 tesla. This is one of several feasible designs satisfying the EuroCirCol specification depending on the number of wedges selected per layer.

the cos-theta current distribution and field quality the blocks must be significantly rotated toward the midplane as seen in the High Field blocks shown in Fig. 2. This also enables another degree of freedom for the turns to be biased toward the minor or major edges. By aligning to the major edge all harmonics are less than 2.9 units.

B. Windability

The greatest challenge for this design is windability and cable stability. The equivalent cable winding strain for the inner layer pole turn is roughly three times greater than the pole turn winding strain for MQXF and may require 'dog bone' bends or mixing between the inner and outer layers. Other FCC designs have the same challenge with strand size and bending radius but with half the number of strands and thus half of the necessary bending force [13]. The inner layer pole turn has large differences between the minor and major bending radii at the ends. This may require additional end part shelves previously employed in the current NbTi IR Quads [21] but not deemed necessary for MQXF design [22]-[23].

The cable size has steadily increased within the LARP framework from 20 strands in SQ to 51 strands in HD2 and this proposal is to use 60 strands.

The idea of an internal Nb_3Sn splice was first successfully tested in the 11 T, cos-theta MSUT dipole at the university of Twente, twenty years ago [24]. Another internal Nb_3Sn splice was also performed at Fermilab in a react-and-wind common coil configuration [25]. This is not currently part of the MQXF expertise but would also be part of continued R&D.

C. Wedge Design

A significant challenge for obtaining the highest field possible is how to effectively fabricate and install wedges with essentially zero inner diameter arc length. Based on MQXF cross sectional analysis, the conductor typically aligns itself with the outer shell diameter. This outer edge alignment also presents a challenge for wedge design since the cable would be 'free' to slide on the wedge surface. This challenge is not unique for this design and is likely a necessary technology advancement for obtaining the highest bore field possible in a cos-theta geometry [14]. A possible solution would be to incorporate wedge and turn positioning directly into the winding mandrel as shown in Fig. 3. This would remove the radial degree of freedom for each turn and place each turn where they naturally gravitate. This feature also would enable traditional wedge fabrication and insulation techniques to be employed.

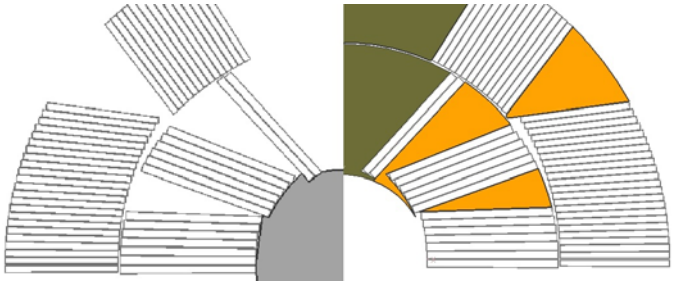

Fig. 3. Two possible solutions to the issue of turn and wedge positioning. For field quality, the conductor must 'lay low' introducing a large degree of radial freedom. The left image shows a modification to the winding mandrel enabling traditional wedge and trace design. The right image demonstrates an intricate wedge profile that would require new insulation techniques.

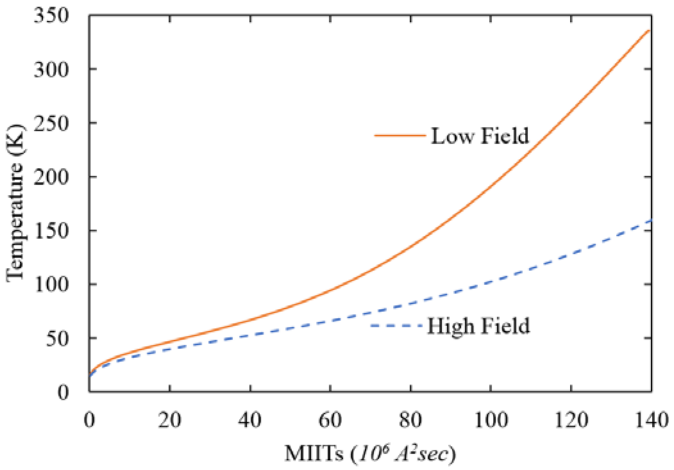

Fig. 4. MIITs curve for the low and high field conductors for a RRR of 150. The peak temperature for the low and high field region is 336 K and 198 K respectively at 105% of I_{nom}. The total quench budget is 140 MIITs or 10^6A^2sec.

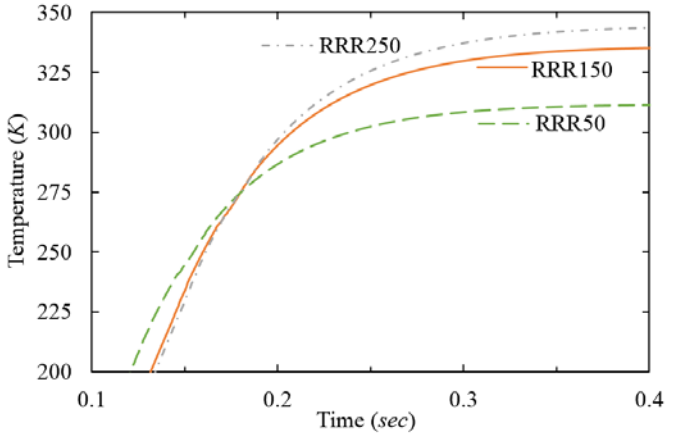

Fig. 5. Low field peak temperature as a function of time after quench for different values of RRR. The listed RRR values are simulated for both low and high field conductors. The energy absorbed by the high field conductor increases with lower RRR values and thus the low field peak temperature decreases with decreased RRR.

IV. Quench Calculation

A. Assumptions

For uniformity across designs, the EuroCirCol quench specification is to determine the peak temperature assuming the entire magnet is completely quenched 40 ms after quench onset. This is a slightly conservative value based on the observed performance of MQXFS1 at nominal current with only protection heaters (10 ms verification, 5 ms circuitry, < 18 ms delay/diffusion) [26]. With Coupled Loss Induced Quench and adequate parameters, essentially an entire magnet can be made normal in roughly 10 ms bringing the time from quench onset to total magnet quench to 25-30 ms [27]-[28]. Regardless, the large inductance and cable size provides current decay times on the order of 150 ms making the rapidity of full magnet quench not as crucial.

The adiabatic quench calculation was performed with the ROXIE quench module [29] using MATPRO materials [30].

B. MIITs and Peak Temperature

The MIITs curve for both conductors is shown in Fig 4. The low field cable has a significantly higher Cu/nonCu ratio. The reduced fraction of superconductor in the low field region significantly increased the peak temperature but remains below 350 K at 105% of I_{nom}.

Counterintuitively the peak temperature actually increases with increased RRR as shown in Fig. 5. The increased resistance causes higher voltage and higher initial temperature. The higher resistance also causes quicker current decay and ultimately lower peak temperature.

C. Peak Voltage to Ground

The resistive and inductive voltage was calculated from the ROXIE quench module [29]. The resistive and inductive response are always opposite each other and the peak voltage difference is 149 volts per meter of magnetic length. If the center lead is grounded the peak voltage to ground for a 15 m long magnet would be 1.105 kV.

V. Conclusion

This two-layer dipole satisfies almost all EuroCirCol specifications. The only non-conformity is the necessary operational current. The design further constricts itself to state-of-the-art rather than future projections of technology. Windability is an open issue for more consideration and R&D but does not intrinsically negate the design.

Next steps would include developing a bladder-and-key support structure to handle preload, cooldown, and Lorentz force. Extensive windability tests are also needed to determine a workable relationship between strand diameter, number of strands and bending radii.

Acknowledgment

The authors would like to thank Carlo Santini, Justin Carmichael, Mattia Parise, Igor Novitski, and Robert Wands for fruitful discussions with simulation, Steve Krave for helpful comments on windability and mandrel image and Lance Cooley for help with conductor capability. A hearty thank you to all members of the LARP collaboration and IB3 crew.

References

[1] E. Todesco *et al*., "Design studies for the low-beta quadrupoles for the LHC luminosity upgrade," *IEEE Trans. Appl. Supercond*., vol. 23, no. 3, June 2013, Art. no. 4002405.

[2] "HL-LHC preliminary design report," CERN-ACC-2014-0300, Nov. 28, 2014.

[3] CERN, "The European strategy for particle physics," CERN, Brussels, Belgium, CERN-Council-S/106, 2013.

[4] D. Tommasini et al., "The 16 T Dipole Development Program for FCC," *IEEE Trans. Appl. Supercond.*, vol. 27, no. 4, June 2017, Art. no. 4000405.

[5] S. Feher *et al*., "Development and test of LARP technological quadrupole (TQC) magnet," *IEEE Trans. Appl. Supercond*., vol. 17, no. 2, pp. 1126–1129, June 2007.

[6] S. Caspi *et al*., "Test and analysis of technology quadrupole shell (TQS) magnet models for LARP," *IEEE Trans. Appl. Supercond*., vol. 18, no. 2, pp. 179–183, June 2008.

[7] G. Ambrosio *et al*., "Design of Nb_3Sn coils for LARP long magnets," *IEEE Trans. Appl. Supercond*., vol. 17, no. 2, pp. 1035–1038, June 2007.

[8] S. Caspi *et al*., "Design of a 120 mm bore 15 T quadrupole for the LHC upgrade phase II," *IEEE Trans. Appl. Supercond*., vol. 20, no. 3, pp. 144–147, June 2010.

[9] F. Borgnolutti *et al*., "Fabrication of a third generation of Nb_3Sn coils for the LARP HQ03 quadrupole magnet," *IEEE Trans. Appl. Supercond*., vol. 25, no. 3, Jun. 2015, Art. no. 4002505.

[10] E. Rochepault *et al*., "Dimensional changes of Nb_3Sn Rutherford cables during heat treatment," *IEEE Trans. Appl. Supercond*., vol. 26, no. 4, June 2016, Art. no. 4802605.

[11] E. F. Holik *et al*., "Fabrication and analysis of 150-mm-aperture Nb_3Sn MQXF coils," *IEEE Trans. Appl. Supercond*., vol. 26, no. 4, June 2016, Art. no. 4000907.

[12] D. Tommasini *et al*., "Baseline Specifications and Assumptions for Accelerator Magnet," [Online]. EuroCirCol-P1-WP5-M5.2 Available: http://cds.cern.ch/record/2150689

[13] D. Tommasini *et al*., "Overview of Magnet Design Options," [Online]. *EuroCirCol-P1-WP5-D5.1* Available: http://cds.cern.ch/record/2226492

[14] M. Sorbi, G. Bellomo, B. Caiffi, P. Fabbricatore, S. Farinon, V. Marinozzi, and G. Volpini, "The EuroCirCol 16T Cosine–Theta Dipole Option for the FCC," *IEEE Trans. Appl. Supercond*., vol. 27, no. 4, June 2017, Art. no. 4001205.

[15] C. Lorin, D. Durante, and M. Segreti, "EuroCirCol 16 T Block-Coils Dipole Option," *IEEE Trans. Appl. Supercond.*, vol. 27, no. 4, June 2017, Art. no. 4001405.

[16] R. Gupta, M. Anerella, J. Cozzolino, W. Sampson, J. Schmalzle, P. Wanderer, J. Kolonko, D. Larson, R. Scanlan, R.J. Weggel, E. Willen, and N. Maineri, "Common Coil Dipoles for Future High Energy Colliders," *IEEE Trans. Appl. Supercond.*, vol. 27, no. 4, June 2017, Art. no. 4000605.

[17] F. Toral, L. Garcia-Tabares, T. Martinez, J. Munilla, J. Ruuskanen, T. Salmi, and A. Stenvall, "EuroCirCol 16 T Common-Coil Dipole Option for the FCC," *IEEE Trans. Appl. Supercond.*, vol. 27, no. 4, June 2017, Art. no. 4001105.

[18] S. Caspi, D. Arbelaez, L. Brouwer, S. Gourlay, S. Prestemon, and B. Auchmann, "Design of a Canted-Cosine-Theta Superconducting Dipole Magnet for Future Colliders," *IEEE Trans. Appl. Supercond.*, vol. 27, no. 4, June 2017, Art. no. 4001505.

[19] C. Sanabria, "A new understanding of the heat treatment of Nb_3Sn superconducting wires." PhD thesis, Dept. of Mat. Sci. & Eng., Florida St. Univ., Tallahassee, CreateSpace Independent Publishing Platform, ISBN 978-1-5447-7013-0, 2017.

[20] C. Sanabria, M. Field, P.J. Lee, H. Miao, D.C. Larbalestier, and J. Parrell, "Reexamining the heat treatment of RRP® Nb_3Sn and the potential for further improvements," *CECICMC 2017*, Madison, WI. M1OrF15 – Contribution ID: 437.

[21] J. Brandt, and A. Simmons, "Coil End Design for the LHC IR Quadrupole Magnet," Fermilab Technical Note# TS-96-013, Fermi National Accelerator Laboratory, Batavia, IL, 1996.

[22] M. Yu, G. Ambrosio, S. Izquierdo Bermudez, R. Bossert, J. Brandt, P. Ferracin, and S. Krave, "Coil End Parts Development Using BEND and Design for MQXF by LARP," *IEEE Trans. Appl. Supercond.*, vol. 27, no. 4, June 2017, Art. no. 4000105.

[23] S. Izquierdo Bermudez, G. Ambrosio, R. Bossert, D. Cheng, P. Ferracin, S.T. Krave, J.C. Perez, J. Schmalzle, and M. Yu, "Coil End Optimization of the Nb_3Sn Quadrupole for the High Luminosity LHC," *IEEE Trans. Appl. Supercond.*, vol. 27, no. 4, June 2017, Art. no. 4001504.

[24] A. den Ouden, S. Wessel, E. Krooshoop and H. ten Kate, "Application of Nb_3Sn Superconductors in High-Filed Accelerator Magnets," *IEEE Trans. Appl. Supercond.*, vol. 7, no. 2, June 1997, pp 733.

[25] V. S. Kashikhin, G. Ambrosio, N. Andreev, E. Barzi, D. Chichili, L. Imbasciati, S. Feher, V. V. Kashikhin, M. Lamm, P. J. Limon, I. Novitski, D. Orris, C. Sylvester, M. Tartaglia, J. Tompkins, S. Yadav, R. Yamada, G. Velev, and A. V. Zlobin, "Development and Test of Single-Layer Common Coil Dipole Wound With Reacted Nb_3Sn Cable," *IEEE Trans. Appl. Supercond.*, vol. 14, no. 2, June 2004, pp 353.

[26] G. Chlachidze *et al*., "Performance of the first short model 150 mm aperture Nb_3Sn quadrupole MQXFS for the High Luminosity LHC upgrade," *IEEE Trans. Appl. Supercond.*, vol. 27, no. 4, June 2017, Art. no. 4000205.

[27] E. Ravaioli, H. Bajas, V.I. Datskov, V. Desbiolles, J. Feuvrier, G. Kirby, M. Maciejewski, G. Sabbi, H.H.J. ten Kate, and A.P. Verweij, "Protecting a Full-Scale Nb_3Sn Magnet With CLIQ, the New Coupling-Loss-Induced-Quench System," *IEEE Trans. Appl. Supercond.*, vol. 25, no. 3., June 2015, Art. no. 4001305.

[28] E. Ravaioli, G. Ambrosio, B. Auchmann, P. Ferracin, M. Maciejewski, F. Rodriguez-Mateos, G.L. Sabbi, E. Todesco, and A.P. Verweij, "Quench Protection System Optimization for the High Luminosity LHC Nb_3Sn Quadrupoles," *IEEE Trans. Appl. Supercond.*, vol. 27, no. 4, June 2017, Art. no. 4702107.

[29] N. Schwerg, B. Auchmann, and S. Russenschuck, "Quench Simulation in an Integrated Design Environment for Superconducting Magnets," *IEEE Trans. On Magn.*, vol. 44, no. 6, June 2008, pp 934.

[30] G. Manfreda, L. Rossi, and M. Sorbi, "MATPRO upgraded version 2012: a computer library of material property at cryogenic temperature," INFN, Milan, Italy, Tech. Rep. *INFN-12-04/MI*, April 2012